A study of the magnetic resonance in a single-crystal $Ni_{50.47}Mn_{28.17}Ga_{21.36}$ alloy

2006 J. Phys.: Condens. Matter 18 7613

(http://iopscience.iop.org/0953-8984/18/32/010)

INSTITUTE OF PHYSICS PUBLISHING JOURNAL OF PHYSICS: CONDENSED MATTER

J. Phys.: Condens. Matter **18** (2006) 7613–7627 doi:10.1088/0953-8984/18/32/010

A study of the magnetic resonance in a single-crystal $Ni_{50.47}Mn_{28.17}Ga_{21.36}$ alloy

V G Gavriljuk[1,3], A Dobrinsky[1], B D Shanina[2] and S P Kolesnik[2]

[1] Institute for Metal Physics, Vernadsky Boulevard 36, UA-03680 Kiev 142, Ukraine
[2] Institute of Semiconductor Physics, Prospect Nauki 45, Kiev 03028, Ukraine

E-mail: gavr@imp.kiev.ua

Received 2 March 2006, in final form 22 June 2006
Published 31 July 2006
Online at stacks.iop.org/JPhysCM/18/7613

Abstract

The single-crystal non-stoichiometric magnetic shape memory alloy $Ni_{1-x-y}Mn_xGa_y$ with $x = 0.2817$, $y = 0.2136$ is studied using magnetic resonance spectroscopy: ferromagnetic resonance (FMR) and conduction electron spin resonance (CESR). The temperature dependence of the integral intensity, the resonance field and the line-width are measured across the wide temperature interval from 4.2 to 570 K. Three phase transformations are found in this alloy: paramagnetic ↔ ferromagnetic with a Curie temperature of 360 K, austenite-to-martensite (direct with $T_{ms} = 312$ K and reverse with $T_{as} = 313$ K), and a transformation at $T = 45$ K, suggestive of the spin-glass state. The angular dependence of the FMR signals is measured in the martensitic and austenitic states before and after the martensite-to-austenite transition. The experimental data are used for determination of the magnetization M_m and anisotropy parameters K_1 and K_2 in the martensitic state. The obtained coefficient K_2 is determined to be not small and, moreover, it is comparable with K_1. The temperature dependence of the resonance signals is also investigated at temperatures significantly higher than T_C, where FMR was transformed to CESR. In the paramagnetic austenitic state (above T_C) the alloy reveals an extremely intensive signal of CESR, which suggests a high concentration of conduction electrons and correlates with the large value of the magnetic-field-induced strain observed in the alloys of such composition. The temperature dependence of the skin layer depth is found from the sharp decay of the CESR signal with temperature, which is related to the disappearing large magnetic resistance after transformation to the paramagnetic state.

[3] Author to whom any correspondence should be addressed.

1. Introduction

Ni–Mn–Ga alloys have been studied extensively since 1996, when the magnetic-field-induced strain (MFIS) was discovered by Ullakko *et al* [1, 2], which suggested a new kind of shape memory effect, namely magnetic shape memory. A mechanism of magnetic shape memory amounts to the field-induced movement of twin boundaries between the martensitic variants which, at the same time, are the magnetic domains [2–4]. Three main conditions are prerequisites for MFIS: (i) a ferromagnetic martensitic structure with the non-cubic distortions of the crystal lattice, which leads to the non-equality of the magnetization axes; (ii) a large enough energy of magnetic anisotropy, so that, for the alignment of the magnetization with the field, the redistribution of twin variants occurs instead of the rotation of magnetic atomic moments; (iii) a sufficiently low stress for twinning, which allows the twin boundaries to move under an applied field of less than 1 T or under a mechanical stress of several MPa.

Webster *et al* [5, 6] were the first to study a correlation between magnetic properties and the crystal structure of Ni_2MnGa alloys. They explained the martensitic transition from the cubic to the tetragonal structure by the discontinuity in the magnetic properties originating from a change in the electron concentration. The maximum magnetic moment (about 4 μ_B per atom [6, 7]) is located at the Mn atoms, whereas Ni atoms carry a significantly smaller magnetic moment ($\sim$0.3 μ_B [6]).

A peculiarity of the magnetic structure is that Ni–Ni and Ni–Mn interatomic exchange interactions have ferromagnetic character, whereas the Mn–Mn exchange interaction is antiferromagnetic between the neighbouring Mn atoms and ferromagnetic if the Mn atoms are separated by the Ni atoms [8, 9]. According to neutron scattering data [10], ferromagnetism in Ni_2MnGa alloys is due to an s–d exchange interaction of RKKY type.

The movement of twin boundaries in Ni_2MnGa is characterized by a low activation enthalpy (of about 0.03–0.04 eV [11]), which is smaller by more than one order than that for the dislocation slip. A reason for such a high mobility of twin boundaries in Ni_2MnGa still remains unclear. The role of the electron structure has so far been discussed in relation to the start temperature of martensitic transformation, T_{ms}. It was shown that T_{ms} increases linearly with the number of valence electrons per atom, e/a [12].

A useful experimental tool for studies of the magnetic and electron structure is the magnetic resonance. The temperature and angular dependence of ferromagnetic resonance (FMR) in the temperature range below the Curie point provides one with knowledge about the nature of magnetization, including magnetic transformations, magnetic sublattices and parameters of magnetic anisotropy. Above the Curie point, one can study conduction electron spin resonance (CESR), which gives information about the electron density at the Fermi level, and it is the more important characteristic in comparison with the e/a ratio.

The aim of this study was to obtain experimental data that could shed light on the role of the electron and magnetic structure in the magnetic-field-induced strain of Ni_2MnGa alloys.

2. Experimental details

The single-crystal, of which the composition, the lattice parameters and the temperatures of phase transformations are given in table 1, was presented by the company Adaptamat Ltd of Espoo, Finland. The martensite in the studied alloy has a tetragonal five-layer crystal structure [13]. Temperatures of phase transitions were obtained due to the measurements of the low-field magnetic susceptibility.

FMR was recorded using electron paramagnetic resonance (EPR) spectrometry in the X-band at the microwave frequency of 9.4 GHz. The magnetic component of the linearly polarized microwave field $\mathbf{H}_1$ is orthogonal to the static magnetic field $\mathbf{H}$ and has a maximum value in the

Table 1. Characteristics of the sample studied.

Content (at.%)			T_{ms} (T_{as})	T_{mf} (T_{af})	T_C	Lattice parameters (Å)/size of the sample (cm)		
Ni	Mn	Ga	(K)	(K)	(K)	*a*	*b*	*c*
50.47	28.17	21.36	312(313)	309(315)	360	5.95/0.6	5.95/0.23	5.59/0.19

centre of the resonator cavity. The equipment permits us to change the external static magnetic field from 0 to 1.3 T. The sample was cut as a rectangular plate with the edges parallel to the crystallographic axes [**100**], [**010**] and [**001**]. The minimal size of the sample coincides with the axis of easy magnetization, ***c***. The sample is put in the centre of the resonator cavity, so that the field **H** is in the plane (**bc**).

Before the measurements, a training treatment was made, i.e. the applied static field was varied several times within its range from 0 to 1.3 T so that, before the measurements, the studied sample mainly consisted of one domain, with the axis of easy magnetisation along the direction of the applied field.

The angular dependence of the FMR signals was measured in the martensitic state at a temperature $T = 290$ K and in the austenitic state at $T = 335$ K. Measurements in the martensitic state were performed in the plane of the magnetic field rotation (**bc**), where **b** is a possible axis and **c** is the axis of easy magnetisation.

The temperature dependence of resonance signals was measured in the temperature range 4.2–570 K.

3. Temperature dependence of the magnetic resonance signals

A common property of FMR absorption in the sample is the significant broadening of the signals. Figure 1 shows the resonance signals recorded at temperatures 4.2 K, 110 K, 300 K (just below T_{ms}), 335 K (above T_{as}) and 570 K (in the paramagnetic state). All the signals are reduced to identical experimental conditions (microwave power, amplification etc).

It is interesting to clarify how the FMR signals change their shape after the phase transformations, because the shape function of the FMR line reflects some electron properties of the alloys. At each temperature, the resonance spectrum was recorded for two magnetic field orientations: $\mathbf{H} \parallel \mathbf{c}$ and $\mathbf{H} \parallel \mathbf{b}$. At $T \geqslant T_{af}$, spectra are close in both orientations. At all temperatures below T_{ms} and at all orientations of the magnetic field, the spectrum is presented by the resonance line having the Lorentzian line-shape and located at a high magnetic field. The theoretical description of all the spectra allows one to obtain the values of the resonance magnetic field, the line-width and the integral intensities.

At temperatures higher than the Curie point, the conduction electron spin resonance was recorded as is seen in figure 1(e).

Figure 2 demonstrates the temperature dependence of the basic parameters for the resonance signal: the resonance field value, $H_{res}(T)$, the line-width, $\Delta H(T)$, and the integral intensity, $I(T)$, across the whole temperature interval. All the signals were recorded on the same scale, i.e. with the same microwave power and amplifying coefficient. Two curves are shown in figure 2: triangular points belong to the case of the magnetic field applied in the direction ***c***, $\mathbf{H} \parallel \mathbf{c}$, and the square points correspond to $\mathbf{H} \parallel \mathbf{b}$. With increasing temperature, these curves reveal a non-monotonous behaviour at temperatures corresponding to the phase transformations. These temperatures are marked with the dash–dotted lines. One can see three transformations.

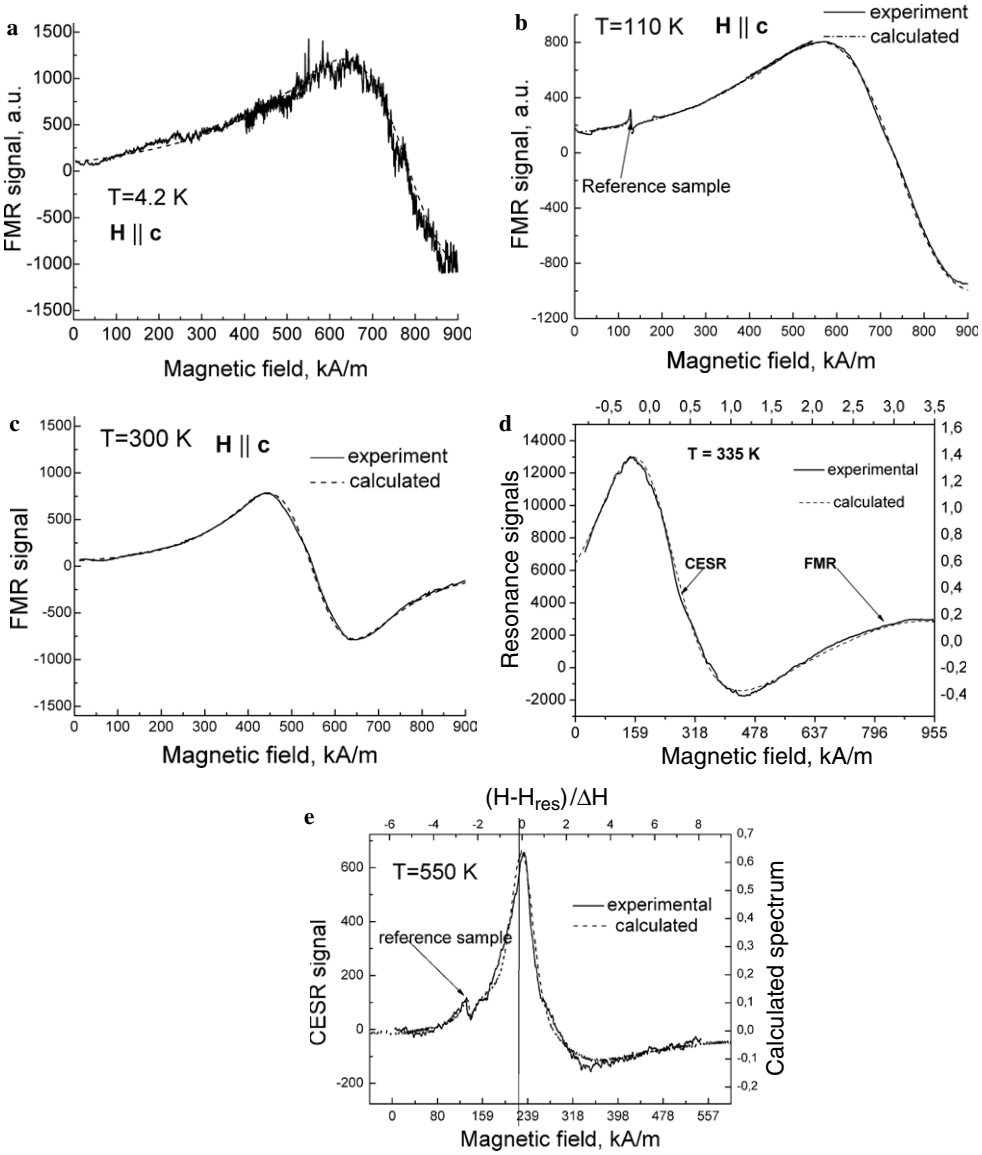

Figure 1. Transformation of the resonance spectrum with the temperature of measurements: (a) 4 K, (b) 110 K, (c) 300 K, (d) 335 K, and (e) 550 K. Solid lines belong to the experimental spectra; dashed lines belong to the calculated spectra.

The first phase transformation occurs at $T = 45$ K. This low-temperature transformation is reflected in the temperature dependence of all spectral parameters, but it is seen especially brightly in the integral intensity of the FMR signal $I(T)$. The FMR signal integral intensity is proportional to the dynamic magnetic susceptibility $\chi_{\mathrm{dyn}}(T)$. It is known [14] that the 'cusp' in the curve $\chi_{\mathrm{dyn}}(T)$ at a low temperature T_{f} is caused by the freezing of spins in the mean field of exchange interaction with variable sign, i.e. by the transformation to the spin-glass state. The temperature T_{f} is named the freezing temperature or the spin-glass transition temperature. We

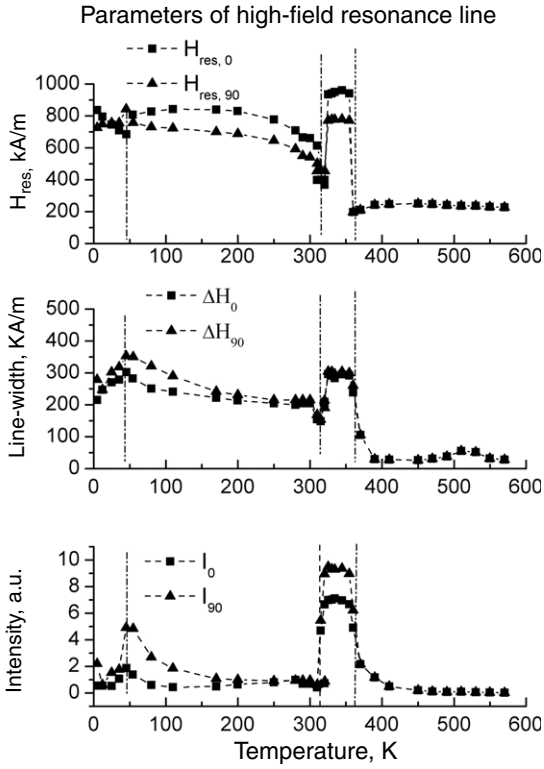

Figure 2. Temperature dependence of the magnetic resonance parameters: the resonance field, the line-width and the integral intensity. $H_{res,0}$ corresponds to $\mathbf{H} \parallel \mathbf{c}$; dash–dotted lines mark the temperature points of phase transformations.

cannot definitely maintain that we observe the spin-glass transition, however it is clear that the disordering in the spin system occurs as soon as the line-width is also broadened at $T = 45$ K.

At $T = 313$–315 K, the system transforms from the martensitic phase to the austenitic phase. The integral intensity of the FMR signal is significantly larger in the austenitic state than in the martensitic state and, for this reason, the $H_{res}(T)$ increases sharply at $T > T_{as}$. The FMR signal is shifted to large values of magnetic field and, simultaneously, a new signal appears (figure 1(d)) which has line-shape specific for the conduction electron spin resonance (CESR), the small line-width, and the very slight angular dependence of H_{res} and ΔH.

More complicated behaviour is observed for the line-width $\Delta H(T)$: just below T_{as}, the line-width decreases and again starts to increase above T_{as}. The decrease in $\Delta H(T)$ before the martensite-to-austenite transformation can possibly be related to the magnetic restructuring accompanying the formation of an adaptive phase in the martensitic state, which is supposed to be formed within the narrow temperature range just below T_{ms} during cooling and, correspondingly, before T_{as} during heating [15].

At $T = 360$ K, the sample undergoes the transformation from the ferromagnetic state to the paramagnetic state.

4. Angular dependence of FMR signal

The Ni_2MnGa martensite is the uniaxial ferromagnetic phase with the axis of easy magnetization $\boldsymbol{c}$ which is one of the crystallographic axes $\langle 001 \rangle$. Correspondingly, the

Table 2. Resonance field and line-width of the FMR signals at $T = 290$ K measured for three directions of the magnetic field along the crystallographic axes.

Resonance fields (T)			Line-width ΔH (T)			Demagnetization factors		
H_c	H_b	H_{60}	$\Delta_c H$	$\Delta_b H$	$\Delta_{60} H$	n_a	n_b	n_c
0.69	0.83	0.57	0.27	0.18	0.30	0.11	0.40	0.49

anisotropic properties of the FMR signal are determined by the values and orientations of magnetic field **H**, saturation magnetization $\mathbf{M}_m$ *(in martensite)* and $\mathbf{M}_a$ *(in austenite)* and the coefficients of anisotropy K_1 and K_2. In the resonance technique, only a single domain is observed because, being out of resonance, other variants are not observed and not needed for studies of the angular dependence of the FMR signal.

If the sample is rotated relative to the direction of the magnetic field, the resonance magnetic field H_{res} and the line-width ΔH of the observable signal change their values, depending on the angle between the magnetic field **H** and the actual crystallographic axis.

The angular dependence of the resonance field $H_{res}(\varphi)$, the line-width ΔH and the integral intensity of the FMR signal were measured for the magnetic field **H** rotating in the crystallographic plane **bc**. The results are presented in figures 3(a)–(c) (martensite) and (d)–(f) (austenite). The difference between the values measured along the **b** and **c** axes reflects their non-equivalence.

Measurements of $H_{res}(\varphi)$ in the crystallographic plane **bc** allow us to find all the magnetic characteristics M_m, K_1, and K_2, taking into account the demagnetization factors of the samples.

In fact, for the determination of the M_m, K_1 and K_2 values, it is enough to know H_{res} for the orientations of the magnetic field in directions **b** and **c**, and in some intermediate direction, e.g. at $\varphi = 60°$. These values for the martensitic state are given in table 2. The demagnetization factors of the samples, which are important for further interpretation of the experimental data, are presented in the last column of table 2.

Figure 3(b) shows the angular dependence of the line-width of the FMR signal defined as the peak-to-peak width on the derivative of the FMR absorption. The angular dependence of the integral intensity in figure 3(c) is similar to that of the line-width, because the amplitude of the signal has a weak and monotonous angular dependence in the interval of $0 < \varphi < 90°$.

If the function $\Delta H(\varphi)$ is similar to the corresponding function $H_{res}(\varphi)$, this suggests that the disorientations of magnetization are small, and the line-width is determined by the scattering of the magnetization values and the values of the exchange interactions over the sample. The clearly different characters of $H_{res}(\varphi)$ and $\Delta H(\varphi)$ in figures 3(a) and (b) mean that the scattering of the magnetization orientations plays an important role in the broadening of the FMR signal in the single-crystal bulk sample.

The austenite in the Ni_2MnGa alloys has the face-centred cubic (fcc) structure. Three cubic axes are magnetically equivalent in the crystal cell, but in the rectangular plates their non-equivalence is determined by the demagnetization factors shown in table 2. The anisotropic properties are determined only by a single coefficient of anisotropy, because the first non-zero K_a is the coefficient of the second order.

The angular dependence of H_{res}, $\Delta H(\varphi)$ and $I(\varphi)$ for the austenitic state was measured at $T = 335$ K. As is seen in figures 3(d)–(f) (see also figure 1(d)), two overlapped resonance lines are observed. One of them (line 1) is typical for the angular dependence of the FMR signal in austenite. The resonance field for this FMR line is large. The low-field line 2 has a weak angular dependence for all three main parameters H_{res}, $\Delta H(\varphi)$ and $I(\varphi)$. The resonance value of the magnetic field for this line is close to the resonance magnetic field for the paramagnetic resonance of conduction electrons. Also taking into account that the line-shape of this

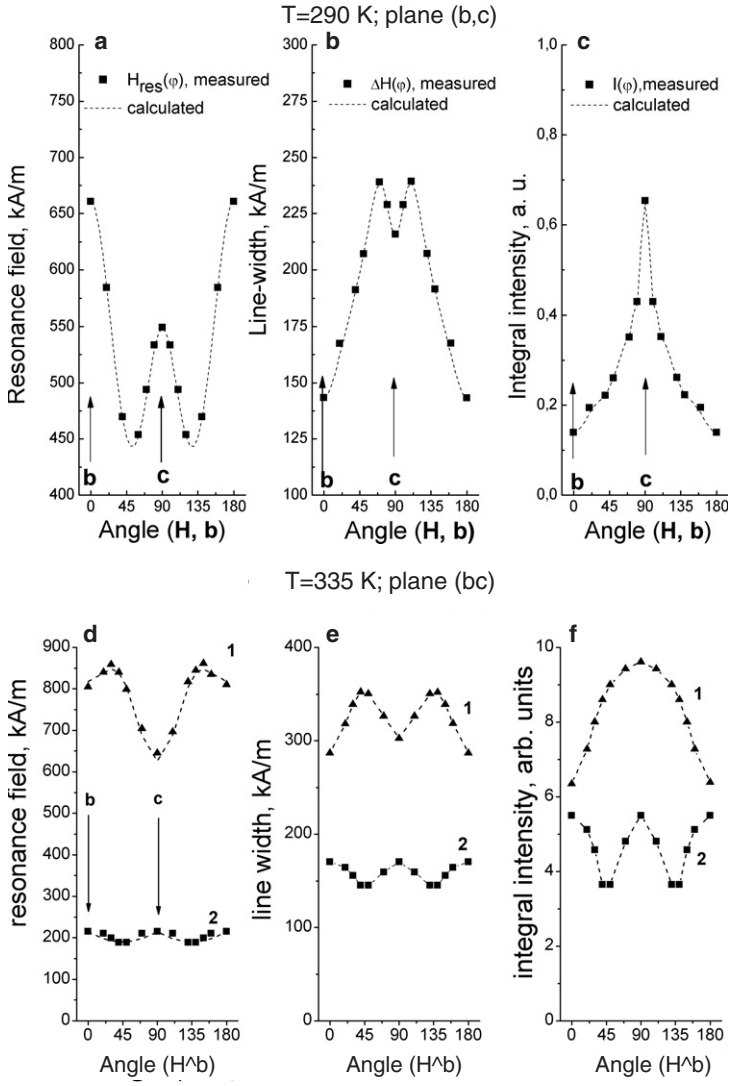

Figure 3. ((a)–(c)) Angular dependence of the resonance field, the line-width and the integral intensity in the martensitic phase measured in the plane (**bc**) (the angle $\varphi = 0$ corresponds to the case of $\mathbf{H} \parallel \mathbf{b}$). ((d)–(f)) Angular dependence of the resonance field, the line-width and the integral intensity for two signals observed in the austenitic state measured in the plane (**bc**) (the angle $\varphi = 0$ corresponds to the case $\mathbf{H} \parallel \mathbf{b}$).

resonance signal is a typical asymmetrical line-shape of the CESR, we attribute this line to the paramagnetic resonance absorption signal for conduction electrons (see in detail section 5.3).

5. Theoretical interpretation of experimental results and discussion

5.1. Angular dependence of the resonance fields

Using the theory presented in our previous study [16], we analysed the experimental angular dependence of the FMR signal parameters in the martensitic state at $T = 290$ K in order to find parameters of magnetic anisotropy.

The free energy of the sample in an external magnetic field **H** is written as [17]:

$$E = -\mu_0 \boldsymbol{H} \cdot \boldsymbol{M} + 0.5\mu_0 M^2 \sum_i n_i m_i^2 + E_{\text{an}} \tag{1}$$

where the first term is the Zeeman energy in magnetic field **H**, which is a vector with the components $\{H\sin\theta\cos\varphi,\ H\sin\theta\sin\varphi,\ H\cos\theta\}$, where θ and φ are spherical coordinates; the second term is the energy of the demagnetization with the factors of demagnetization n_i for a rectangular sample such as the three-axial ellipsoid; $\mathbf{m}_i$ are unit vectors of the sample magnetization $(\sin\theta_1\cos\varphi_1,\ \sin\theta_1\sin\varphi_1,\ \cos\theta_1)$; μ_0 is the magnetic constant; and E_{an} is the energy of anisotropy.

In case of the ferromagnetic sample with the easy axis of the magnetisation $\boldsymbol{c}$ (the martensitic state), the energy of anisotropy is [17]

$$E_{\text{an},m} = -K_1(mc)^2 + K_2(mc)^4, \tag{2}$$

where K_1 and K_2 are parameters of anisotropy of the first and second orders, respectively.

The parameter of anisotropy K_1 in formula (2) has the sign opposite to that of K_{u}, the value of which was determined in many studies of the Ni_2MnGa alloys from the measurements of magnetization curves (see e.g. [18]). Our determination of K_1 is in accordance with [17] and it means that the alignment of M in direction c decreases the free energy.

In the cubic lattice (austenitic state) the crystallographic axes are equivalent for the magnetization alignment, and the energy of anisotropy is determined by the following equation:

$$E_{\text{an},a} = K_{\text{a}}(m_1^2m_2^2 + m_1^2m_3^2 + m_2^2m_3^2). \tag{3}$$

The equilibrium orientation of the magnetization in relation to the applied magnetic field is found from the first derivatives of the free energy (1), putting them to be equal to zero:

$$\frac{\partial E(\theta_1,\varphi_1,\theta,\varphi)}{\partial\theta_1} = 0; \qquad \frac{\partial E(\theta_1,\varphi_1,\theta,\varphi)}{\partial\varphi_1} = 0. \tag{4}$$

The resonance values of the magnetic field are solutions of the following equation containing the second derivatives of the free energy (see [19, 20]):

$$\left(\frac{\Omega}{\gamma}\right)^2 = \frac{1}{M_{\text{m}}^2\sin^2\theta_1}\left[\frac{\partial^2E}{(\partial\theta_1)^2}\frac{\partial^2E}{(\partial\varphi_1)^2} - \left(\frac{\partial^2E}{\partial\theta_1\partial\varphi_1}\right)^2\right]. \tag{5}$$

Taking into account (1)–(4), the equation (5) can be written in the general case as

$$(H_{\text{res}} + f_1(\varphi))(H_{\text{res}} + f_2(\varphi)) - (\Omega/\gamma)^2 = 0, \tag{6}$$

where Ω is the microwave field frequency, and γ is the gyromagnetic ratio of the electron in the alloy, so that $(\Omega/\gamma) = 0.3211$ T.

For the case of martensitic state and magnetic field **H** in the plane (**bc**) (**c** $\parallel$ y; **b** $\parallel$ x; **a** $\parallel$ **z** $\parallel$ $\mathbf{H}_1$), the functions $f_1(\varphi)$ and $f_2(\varphi)$ are found as

$$\begin{aligned} f_1^{(\text{m})} &= -b_2 + \cos^2\varphi(A_1 + A_2 + b_1) - A_2\cos^4\varphi, \\ f_2^{(\text{m})} &= -(A_1 + A_2 + b_1) + (2A_1 + 2b_1 + 5A_2)\cos^2\varphi - 4A_2\cos^4\varphi. \end{aligned} \tag{7a}$$

Respectively, for the case of austenite

$$\begin{aligned} f_1^{(\text{a})} &= -(b_2 - A_{\text{a}}) + (b_1 - 2A_{\text{a}})\cos^2\varphi + 2A_{\text{a}}\cos^4\varphi, \\ f_2^{(\text{a})} &= -b_1 + A_{\text{a}} + (2b_1 - 8A_{\text{a}})\cos^2\varphi + 8A_{\text{a}}\cos^4\varphi, \\ b_2 &= 4\pi M_{\text{m}}(n_{\text{c}} - n_{\text{a}}); \qquad b_1 = 4\pi M_{\text{m}}(n_b - n_{\text{c}}). \end{aligned} \tag{7b}$$

The values of n_{i} are given in table 2; the fields of anisotropy $A_1 = 2K_1/M_{\text{m}}$, $A_2 = 4K_2/M_{\text{m}}$, and $A_{\text{a}} = 2K_{\text{a}}/M_{\text{a}}$.

Table 3. Magnetic parameters of the alloy studied at temperature $T = 290$ K for martensite and $T = 335$ K for austenite.

M_m (A m^2 kg^{-1})	A_1 (kA m^{-1})	A_2 (kA m^{-1})	K_1 (10^5 J m^{-3})	K_2 (10^5 J m^{-3})	M_a (A m^2 kg^{-1})	A_a (kA m^{-1})	K_a (10^5 J m^{-3})
112	−87.6	366	−0.5	1.04	220	159.2	1.8

By solving equation (6), one obtains the angular dependence of the resonance field H_{res}:

$$H_{res}^{(j)}(\varphi) = -0.5(f_1^{(j)} + f_2^{(j)}) + [0.25(f_1^{(j)} - f_2^{(j)})^2 + 0.3211^2]^{1/2}. \quad (8)$$

The large value of $H_{res}(\varphi)$ in figure 3(a) concerns large values of the magnetization and of the asymmetry parameter. The values of M_m, K_1 and K_2 are found from the fitting of formulae (7*a*) and (8) to the experimental data of figure 3(a).

The magnetic anisotropy of the alloy in its austenitic state, A_a, and the value $4\pi M_a$ are determined from the fitting of (7*b*) and (8) to the data for the FMR signal 2 from figure 3(d). All the constants are given in table 3.

The obtained constant of anisotropy in the austenitic phase K_a is larger than that in [21] by two orders and larger than those obtained in our study [15] by about one order. A reason for this variance lies in the different compositions studied, e.g. the increased Ni content in [21] should decrease the magnetic anisotropy (compare the value of 5×10^3 J m^{-3} obtained in [21] with 4.9×10^2 J m^{-3} for the pure Ni [17]).

It follows from the data obtained that the martensitic single crystal is characterized by large values of the anisotropy parameters of the first and second orders. The obtained large values of the both parameters K_1 and K_2 show how strong the magnetic anisotropy is in the alloy studied and explain why the magnetic domains coincide with the martensitic variants. Let us compare the result obtained with the data of magnetic anisotropy K_u obtained from the measurements of the magnetization curves and called 'the anisotropy coefficient of the first order' [22]. As shown in our previous study [16], the constant K_u is linked to the fundamental constants through the combination $K_u = 2K_2 - K_1$. The value $K_u = 2.65 \times 10^5$ J m^{-3} from [22] is consistent with $2K_2 - K_1 = 2.58 \times 10^5$ J m^{-3} obtained in our measurements.

This experimental result is consistent with our previous data on K_1 and K_2 in several Ni_2MnGa alloys [16], and it is at variance with the theoretical calculations [23, 24] where a negligibly small value of K_2 was obtained.

The authors [23, 24] attribute the difference between their theoretical results and experimental values [16], in particular the large value of K_2, to an average on different twins whose easy axes are orthogonal to each other. We are forced to give some comments on this statement.

First, in our previous study [16], as well as in the current work, we did not measure any average FMR values. The geometry of the experiment is such that the microwave excitation is possible only in one domain with the polarization of atomic spins parallel to the applied static field H of 0–1.3 T and orthogonal to the microwave field H_1 with a frequency of 9.4 GHz. If we imagine that it could be possible to excite two twin domains, then two different resonance signals with different resonance magnetic fields and absolutely different angular dependence should be observed. Moreover, while rotating the static magnetic field, the FMR signal for the domain with the initial parallel orientation of magnetization would decrease, whereas the signal of the orthogonal domain would increase. We never observed two signals with these expected characteristics.

Second, the theoretical study [23, 24] deals with the stoichiometric Ni_2MnGa composition of high symmetry. Any divergences of symmetry due to deviations from the stoichiometry

cause a change in the angular dependence of the anisotropy energy on the orientation of magnetization, so that the theoretical curve $E(\theta)$ cannot have an ideal character like the one obtained in [23, 24]. The attempt to calculate the magnetic anisotropy for the non-stoichiometric alloy $Ni_2Mn_{1.25}Ga_{0.75}$ [25] is also related to an ideal situation where the excessive Mn atoms substitute symmetrical positions of Ga atoms in the crystal lattice.

Third, the anisotropy parameter K_1 in the alloy studied cannot be so large, $K_1 = 170\ \mu\text{eV} \sim 10^7\ \text{J m}^{-3}$, as is calculated in [25]. The ferromagnetic resonance signal was recorded for external static magnetic fields of 0–1.3 T. As mentioned above (see section 2), due to the training treatment, the sample consists of one domain with the axis of easy magnetization parallel to the direction of the applied field. The value of the resonance magnetic field is determined by the Zeeman energy, demagnetization energy and anisotropy energy. If K_1 would have the values calculated in [23, 24], the resonance signal should fall into the negative range of the magnetic field values and would never be observed. However, in the experiment, the FMR signal is always located at magnetic fields of about 0.5–0.7 T.

5.2. Angular dependence of the line-width

The broadening of the FMR line-width can be caused by the following factors: (i) the magnon damping, $\Delta H^{(0)}$, due to the exchange interaction between magnetic moments; (ii) the scattering of the magnetization values and the values of the anisotropy parameters K_1 and K_2; (iii) a small disorientation of the magnetization vector and of the vector of easy magnetization. The first contribution does not depend on the angle between the sample magnetization and crystallographic axes, however other contributions are angle-dependent. If the dispersion of the internal magnetic field values $H_\text{i} = 4\pi M_\text{m}(n_\text{i} - n_j) + A_1 + A_2$ is the main reason for the broadening of the FMR line, its angular dependence should be similar to that of the resonance field $H_\text{res}(\varphi)$. In the case of a large contribution from the **M** disorientation, the angular dependence of $\Delta H(\varphi)$ should be strongly distinguished from that for $H_\text{res}(\varphi)$ where φ is the angle between **M** and the actual crystallographic axis. The latter case is observed in figures 3(a) and (b).

Let us expand $\Delta H(\varphi)$ to small deviations δB, δA and $\delta\varphi$ to the second order

$$\Delta H(\varphi) = \Delta H^{(0)}(\varphi) + \sum_{j=1,4} \langle(\delta x_j)^2\rangle \left(\frac{\partial^2(\Delta H)}{\partial x_j^2}\right) \tag{9}$$

where $x_1 = M_\text{m}$, $x_2 = A_1$, $x_3 = A_2$ and $x_4 = \varphi$, and $\langle(\delta x_j)^2\rangle = \langle(x_j - x_{j0})^2\rangle$ means the variance of x_j. The odd terms in δx_j are absent, because they disappear on being averaged over the sample.

Let $H_\text{res} = H_\text{res}^{(0)} + D$, where D is a random deviation of H_res in some points of the sample. If the contribution of the scattering of H_res into the broadening of the resonance signal prevails, it can be shown for a Lorentzian shape of line and in the case of $D \gg \Delta H^{(0)}$ that the broadened line-width is approximately equal to the value of D: $\Delta H = \Delta H^{(0)}(1 + (D/\Delta H^{(0)})^2)^{1/2} \approx D$. It allows us to consider approximately that

$$\partial^2(\Delta H)/(\partial x_j)^2 \approx \partial^2(H_\text{res})/(\partial x_j)^2.$$

By differentiating equation (6) on x_j, after some simple calculations one finds $\partial^2(H_\text{res})/(\partial x_j)^2$ as a function of $H_\text{res}(\varphi)$, $f_{1,2}(\varphi)$, and $\partial^2(f_{1,2}(\varphi))/(\partial x_j)^2$, where f_1 and f_2 are given in (7*a*). The theoretical function $\Delta H(\varphi)$ is obtained as the following:

Table 4. Deviations of the values of the magnetic parameters, as estimated from the angular dependence of the FMR line-width.

$\Delta H^{(0)}$ (T)	$(\delta M)_{\rm rms}$	$(\delta A_2)_{\rm rms}$	$(\delta A_1)_{\rm rms}$	$(\delta\varphi)_{\rm rms}$ (deg)
0.21	0.25	0.6	0	2.7

$$\begin{aligned}\Delta H(\varphi) = \Delta H^{(0)} + \frac{\langle\delta M_{\rm m}^2\rangle}{M_{\rm m}^2}[&2A_1(F_1\sin^2\varphi - \cos^2\varphi)\\ &+ 2A_2(F_1\sin^2\varphi - (0.25F_2 + F_1)\sin^2 2\varphi) + F_3(-4\pi M_{\rm m}(n_b - n_{\rm a})\\ &+ (4\pi M_{\rm m}(n_b - n_{\rm c}) - A_1)\sin^2\varphi - A_2\sin^2\varphi(1 - 3\cos^2\varphi))^2]\\ &+ \frac{\langle\delta A_1^2\rangle}{A_1^2}F_3A_1^2\sin^4\varphi + \frac{\langle\delta A_2^2\rangle}{A_2^2}F_3A_2^2\sin^4\varphi(1 - 3\cos^2\varphi)^2\\ &+ \langle\delta\varphi^2\rangle[2H_{\rm i}(1 + F_1)\cos 2\varphi + 2A_2(1 + 3F_1)(\sin^2 2\varphi - 2\cos 2\varphi\cos^2\varphi)\\ &+ F_3\sin^2 2\varphi(H_{\rm i} - 3A_2\cos 2\varphi)^2]. \end{aligned} \tag{10}$$

$H_{\rm i} = 4\pi M_{\rm m}(n_b - n_{\rm c}) + A_1 + A_2$ is an internal magnetic field in the sample;

$$F_1 = \frac{H_{\rm res} + f_1}{2H_{\rm res} + f_1 + f_2}; \qquad F_2 = \frac{H_{\rm res} + f_2}{2H_{\rm res} + f_1 + f_2}; \qquad F_3 = \frac{2F_1F_2}{2H_{\rm res} + f_1 + f_2}. \tag{11}$$

The line in figure 3(b) presents the fitting results of the calculated $\Delta H(\varphi)$ from (10), (11) to the experimental data. The root mean square deviation values $(\delta M_{\rm m})_{\rm rms} = (\langle\delta M_{\rm m}^2\rangle/M_{\rm m}^2)^{0.5}$, $(\delta\varphi)_{\rm rms} = (\langle\delta\varphi^2\rangle)^{0.5}$, $(\delta A_1)_{\rm rms} = (\langle\delta A_1^2\rangle/A_1^2)^{0.5}$, and $(\delta A_2)_{\rm rms} = (\langle\delta A_2^2\rangle/A_2^2)^{0.5}$, and the value of the the magnon damping constant $\Delta H^{(0)}$ are given in table 4. As is seen, the contribution of scattering of the first-order anisotropy field $(\delta A_1)_{\rm rms}$ to the FMR line-width is absent. The second-order anisotropy field A_2 reveals a huge dispersion. The single crystal reveals also a large scattering of the values of magnetization and of its orientations.

5.3. Electron properties

Some useful information concerning the conduction electrons can be obtained from the analysis of the CESR spectra measured at temperatures higher than the Curie temperature $T_{\rm C}$ where only conduction electrons contribute to the spectrum. It was shown in our previous study [16] that there is a correlation between the concentration of conduction electrons and the value of the magnetic-field-induced strain obtained for a set of alloys.

First, an important role of the electron concentration can be concerned with the stability of austenite in relation to the martensitic transformation, as was discussed by Webster *et al* [6]. The role of free electrons in driving the martensitic transformation in the Ni_2MnGa alloy was also demonstrated by Ruskin [26] who added vanadium to this alloy, which reduced the radius of the Fermi sphere and thereby inhibited the martensitic transformation. It is natural to expect that, with increasing concentration of free electrons, thermodynamic stability of the austenitic phase can be diminished. Thus, the search for compositions characterized by the increased concentration of conduction electrons and, correspondingly, by the crystal structure unstable in relation to structural transformations is the promising approach to the development of new MSM alloys.

Second, the concentration of free electrons should affect the mobility of interfaces between martensitic variants which are the twin boundaries. The point is that the mobility of dislocations, including the twinning ones, is controlled by their energy per length unit, i.e. by the line tension Γ which is proportional to the shear modulus μ, $\Gamma \sim \mu b^2$, where b

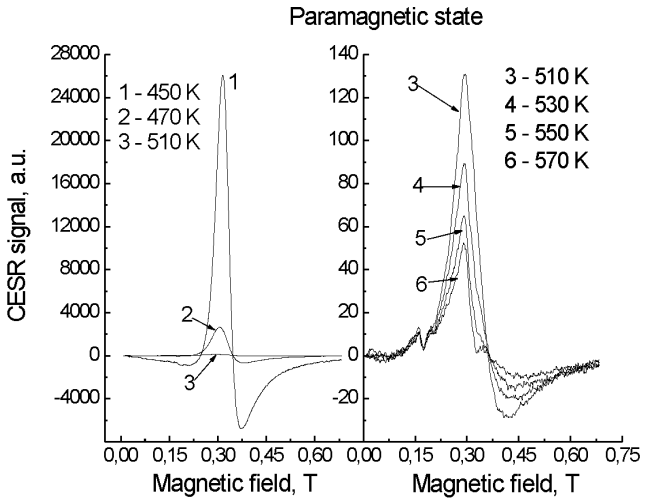

Figure 4. High-temperature spectra in the paramagnetic state of the sample recorded at $T > T_c$, where T_c is the Curie temperature for the ferromagnetic–paramagnetic transformation.

is the Burgers vector. The larger the concentration of free electrons, the more pronounced the metallic character of interatomic bonds and, consequently, the smaller the expected shear modulus. The magnetic-field-induced strain in Ni_2MnGa alloys occurs due to twinning under stress developed by the applied magnetic field (smaller than 2–3 MPa). This abnormally low twinning stress is evidence of the low shear modulus, and it is reasonable to suggest that it is provided by a high concentration of free electrons.

Let us estimate the concentration of free electrons in the studied alloy using the data of conduction electron spin resonance. The line-shape and the asymmetry of the signals recorded at temperatures higher than the Curie point (see figure 4) are specific for electron spin resonance of the degenerate system of free electrons (conduction electron spin resonance, CESR). The small peak at the low magnetic field value is related to the reference sample (a piece of the borate glass containing the number of spins $N_r = 4 \times 10^{15}$). The signals are surprisingly large. One can see that the amplitude of the resonance signal sharply decays with increasing temperature. This fact is attributed to the temperature dependences of the conductance and the conduction electron diffusion rate. We have described the experimental signals using the theory of CESR developed in [27]. The microwave field penetrates the metallic sample to the depth δ, named the skin layer. Being excited by the microwave field, the electron moves through the skin layer into the bulk of the sample carrying the excitation during the spin relaxation time. As the line-shape of the CESR is determined by the ratio T_D/T_2, where T_D is the time of the electron diffusion through the skin layer, T_2 is the spin relaxation time, and the visible amplitude is proportional to $(T_D/T_2)^2$, there is a possibility of finding the temperature dependence of (T_D/T_2). Using the theory [27], the theoretical resonance line was fitted to the experimental signal, as is shown in figure 5. Due to the fitting, we have found the $(T_D/T_2)^2$, the resonance magnetic field, the line-width and the integral intensity in comparison with the integral intensity of the ESR for the reference sample. The concentration of conduction electrons was found from the next relation [27]:

$$N_e = (4/3)(P_s/P_{ref})(E_F/kT)N_r/V_s \tag{9}$$

where P_s and P_{ref} are the integral intensities of the CESR signals in the Ni_2MnGa and reference

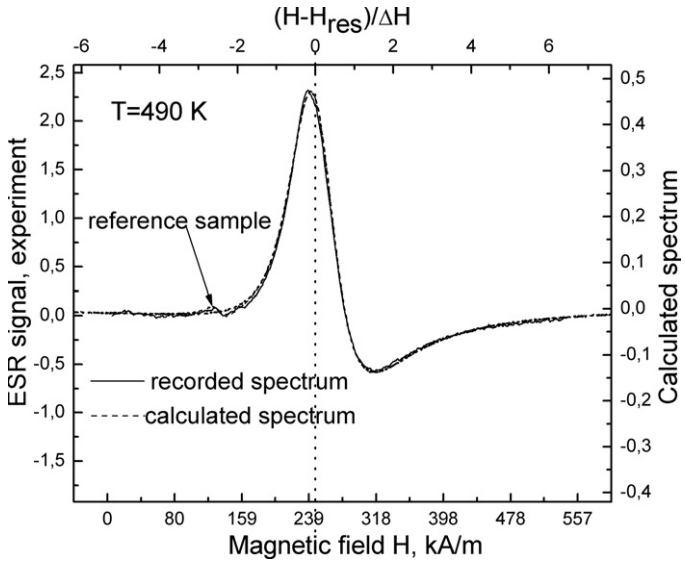

Figure 5. The theoretical description of the conduction electron spin resonance in the paramagnetic state of the sample.

samples, respectively; E_F is the Fermi energy for Ni_2MnGa; V_s is the volume of the sample; and N_r is the number of spins in the reference sample. The obtained N_e is 1×10^{22} cm^{-3}. Such a large concentration of free electrons is comparable, e.g. with those obtained in the hydrogen-charged iron-based alloys [28, 29] where hydrogen is found to increase the density of electron states at the Fermi level significantly, which results in the phenomenon of hydrogen-enhanced localized plasticity.

Let us also discuss a reason for the sharp decay of the CESR signal amplitude with increasing temperature, which is due to the temperature dependence of the ratio $R = (\delta/\delta_e)^2 = (T_D/T_2)^2$, where δ is the skin-layer depth and δ_e is the conduction electron path for the spin relaxation time (see figure 6). The spin relaxation time can only decrease with increasing temperature and therefore it cannot be responsible for the decay of the $R(T)$ with increasing temperature. At the same time, the squared depth of the skin layer, $\delta^2 = (c/4\pi)(\omega\sigma)^{-1}$, is proportional to the resistivity of the sample (where c is the light velocity in the material studied, ω is the frequency of the microwave field, and σ is the conductance of the sample). Therefore, the experimental decay of $R(T)$ with temperature represents the decrease of the high-frequency resistivity. A 20-fold change in $R(T)$ within the temperature interval from 450 to 570 K allows us to suppose that a giant magneto-impedance occurs in the ferromagnetic $Ni_{50.47}Mn_{28.17}Ga_{21.36}$ alloy. The experimental curve is described approximately as $R(T) = 10^{-3.97} \exp(3967/T)$. The exponential law of the impedance decay with temperature can be explained by the weak localization of the electrons on the magnetic moments due to exchange interaction and by the ionization of electrons with increasing temperature. The activation energy $\varepsilon = k_B 3967$ (± 10 K) $= 0.34(\pm 0.001)$ eV characterizes the ionization energy of the localized electron state at fluctuations of the magnetic moment.

It is remarkable that the component of the conduction electrons is also observed in the spectra of the ferromagnetic austenite (figures 1(d), 3(d)–(f)). This signal is recorded at magnetic fields significantly smaller than those for the FMR signal corresponding to the magnetic saturation of austenite.

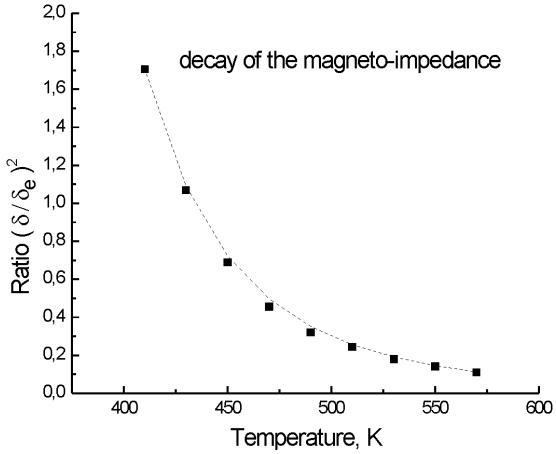

Figure 6. Temperature dependence of the ratio $R = (\delta/\delta_D)$ which determines the asymmetry of the CESR signal; points are the experimental data; the dashed line is the exponential function $R = 10^{-3.97}\exp(3967/kT)$.

Let us test the reasonableness of its interpretation by the estimation of the resonance field value for CESR in the ferromagnetic austenite. At small applied fields, there are three kinds of equivalent magnetic domains [100], [010], [001] with equal volumes. If $H \parallel [100]$, two kinds of domains orthogonal to **H** have no magnetic polarization and only [100] domains are magnetized, but with the value of magnetization significantly smaller than the saturation magnetization. At the microwave frequency used, conduction electrons have a resonance magnetic field value equal to $H_0 = 0.34$ T in the range of the non-polarized domains and the shifted value $H_{res} = H_0 - H_i$ in the domains of [100] kind, where H_i is the intrinsic magnetic field in the domain. Since the electron is moving over the sample, this causes the averaging of the above resonance field values (known as 'motion narrowing'). As a result, the resonance magnetic field for CESR can be written as $H_{res}(0) = (3H_0 - H_i)/3 = H_0 - 0.33H_i$. From comparison with the experimental value of $H_{res}(0) = 0.27$ T, we obtain $H_i = 0.21$ T. If the magnetic field is rotated from the [100] to the [010] direction, the second domain is involved and the shift of H_{res} has its maximum at $\varphi = 45°$: $H_{res}(45°) = (3H_0 - 2^{1/2}H_i)/3 = H_0 - 0.47H_i$. Substituting $H_i = 0.21$ T, we obtain $H_{res}(45°) = 0.24$ T, which corresponds to the experimental data in figure 3(d), curve 2.

Thus, because of the cubic lattice, the occurrence of the CESR along with the FMR signal is the inherent feature of the ferromagnetic austenite. A large intensity of CESR is evidence of the high density of conduction electrons, which in our opinion belongs to fundamental properties determining the magnetic-field-induced strain in Ni_2MnGa alloys.

Summary

The FMR study of the non-stoichiometric single-crystal alloy $Ni_{50.47}Mn_{28.17}Ga_{21.36}$ leads to the following conclusions concerning its magnetic and electronic properties:

(1) It is confirmed that the strong magnetic anisotropy is characterized by the large values of both coefficients of magnetic anisotropy, K_1 and K_2.
(2) A new phase transformation is observed at $T = 45$ K. We suppose that the sample undergoes spin-glass transformation. Some additional experiments have to be performed to test this assumption.

(3) The alloy is characterized by a large disordering of the magnetization orientations, which follows from the difference in the angular dependences of the resonance field and of the line-width.
(4) The values of the FMR resonance field increase abruptly during the martensite-to-austenite transformation, which is concerned with a higher magnetization of austenite at the applied fields that is smaller than those for magnetic saturation.
(5) The large value of the concentration of conduction electrons, as obtained from CESR measurements at temperatures higher than the Curie point, suggests a small shear modulus and, correspondingly, a small line tension of twinning dislocations, which can be a reason for the high mobility of twin boundaries and makes possible the strain under low mechanical stress provided by the applied magnetic field.
(6) The temperature dependence of the CESR integral intensity reveals a giant magneto-impedance in the ferromagnetic phase and its exponential decay in the paramagnetic state.

Acknowledgment

The authors thank Dr K Ullakko, Adaptamat Ltd, Espoo, Finland, for the single-crystal used in this study.

References

[1] Ullakko K 1996 *J. Mater. Eng. Perform.* **5** 405
[2] Ulakko K, Huang J K, Kantner C, O'Handley R C and Kokorin V V 1996 *Appl. Phys. Lett.* **69** 1966
[3] Handley R C 1998 *J. Appl. Phys.* **83** 3263
[4] Likhachev A A and Ullakko K 2000 *Eur. Phys. J.* B **14** 263
[5] Webster P J 1968 *Doctor Thesis* University of Sheffield
[6] Webster P J, Ziebeck K R A, Town S L and Peak M S 1984 *Phil. Mag.* B **49** 295
[7] Ooiwa K, Endo K and Shinogi A 1992 *J. Magn. Magn. Mater.* **104–107** 2011
[8] Caroli B and Blandin A 1966 *J. Phys. Chem. Solids* **27** 503
[9] Enkovara J, Heczko O, Ayuela A and Nieminen R M 2003 *Phys. Rev.* B **67** 212405
[10] Ishikawa Y and Noda Y 1974 *Solid State Commun.* **15** 833
[11] Gavriljuk V G, Soederberg O, Bliznuk V V, Glavatska N I and Lindroos V 2003 *Scr. Mater.* **49** 803
[12] Wuttig M, Liu L, Tsuchiya K and James R D 2000 *J. Appl. Phys.* **87** 4707
[13] Glavatska N, Mogilny G, Danilkin S and Hohlwein D 2003 *Mater. Sci. Forum, EPDIC-8* **443** 397
[14] Korenblit I Ya and Shender E F 1989 *Usp. Fiz. Nauk* **157** 267 (in Russian)
[15] Glavatska N, Mogylny G, Glavatsky I, Tyshchenko A, Soderberg O and Lindroos V K 2002 *Mater. Sci. Forum* **394/395** 537
[16] Shanina B D *et al* 2001 *J. Magn. Magn. Mater.* **237** 309
[17] Vonsovsky S V 1971 *Magnetism* (Moscow: Nauka) p 667 (in Russian)
[18] Handley R C, Murray S J, Marioni M, Nembach H and Allen S M 2000 *J. Appl. Phys.* **87** 4712
[19] Artman J O 1957 *Phys. Rev.* **105** 62
[20] Smith J and Beljers H C 1955 *Philips Res. Rep.* **10** 113
[21] Tickle R and James R D 1999 *J. Magn. Magn. Mater.* **195** 627
[22] Heczko O, Straka L, Lanska N and Ullakko K 2002 *J. Appl. Phys.* **91** 8228
[23] Enkovaara J, Ayuela A, Nordström L and Nieminen R M 2002 *J. Appl. Phys.* **91** 7798
[24] Enkovaara J *et al* 2004 *Mater. Sci. Eng.* A **378** 52
[25] Enkovaara J, Heczko O, Ayuela A and Nieminen R M 2003 *Phys. Rev.* B **67** 212405
[26] Ruskin L S 1980 *MSc Thesis* Salford University
[27] Gavriljuk V G *et al* 1993 *Phys. Rev.* B **48** 3224
[28] Gavriljuk V G, Shivanyuk V N and Foct J 2003 *Acta Mater.* **51** 1293
[29] Gavriljuk V G, Shivanyuk V N and Shanina B D 2005 *Acta Mater.* **53** 5017